IRSTI 30.17.02

*A. Issakhov, A. Abylkassymova, M. Sakypbekova

Faculty of Mechanics and Mathematics, al-Farabi Kazakh National University,
Almaty, Kazakhstan
*e-mail: alibek.issakhov@gmail.com

Applications of parallel computing technologies for modeling the mixed convection in backward-facing step flows with the vertical buoyancy forces

Abstract. This paper presents numerical solutions of the mixed convection in backward-facing step flows with the vertical buoyancy forces. A two-dimensional incompressible Navier-Stokes equation is used to describe this process. This system is approximated by the control volume method and solved numerically by the projection method. The two-dimensional Poisson equation satisfying the discrete continuity equation that is solved by the Jacobi iterative method at each time step. The numerical solutions of the laminar flow behind the backward-facing step with the vertical buoyancy forces are compared with the numerical results of other authors. This numerical algorithm is completely parallelized using various geometric domain decompositions (1D, 2D and 3D). Preliminary theoretical analysis of the various decomposition methods effectiveness of the computational domain and real computational experiments for this problem were made and the best domain decomposition method was determined. In the future, a proven mathematical model and parallelized numerical algorithm with the best domain decomposition method can be applied for various complex flows with the vertical buoyancy forces.

Key words: domain decomposition method, backward-facing step flow, projection method, vertical buoyancy forces, mixed convection.

Introduction

In many technical flows of practical interest, like flow divisions, with the sudden expansion of geometry or with subsequent re-joining, are a common occurrence. The existence of a flow separation and recirculation area has a significant effect on the performance of heat transfer devices, for example, cooling equipment in electrical engineering, cooling channels of turbine blades, combustion chambers and many other heat exchanger surfaces that appear in the equipment.

Many papers are devoted to the motion of a fluid with separation and reconnection of flows without taking into account the buoyancy forces. The importance of this process is indicative of the number of papers where special attention was paid to building equipment [1-3] and developing experimental and theoretical methods for detailed study of flows with separation regions [4-6]. An extensive survey of isothermal flows in fluid flows is given in papers [10-12]. Heat transfer in the flows has been investigated by many authors, like Aung [13, 14], Aung et al. [15], Aung and Worku [16], Sparrow et al. [17, 18] and Sparrow and Chuck [19]. However, published papers on this topic do not take into account the strength of buoyancy force on the flow stream or the characteristics of heat transfer. These effects become significant in the laminar flow regime, where the velocity is relatively low, and when the temperature difference is relatively high. Ngo and Byon [26] studied the location effect of the heater and the size of the heater in a two-dimensional square cavity using the finite element method. Oztop and Abu-Nada [27] numerically investigated natural convection in rectangular shells, partially heated from the side wall by the finite volume method.

In this paper considered the influence of buoyancy forces on the flow and heat transfer

characteristics in individual flows. Numerical solutions for a laminar mixed convective airflow (Pr=0.7) in a vertical two-dimensional channel with a backward-facing step to maintain the buoyancy effect are shown in Figure 1. Numerical results of interest, such as velocity and temperature distributions, re-binding lengths and friction coefficients are presented for the purpose of illustrating the effect of buoyancy forces on these parameters.

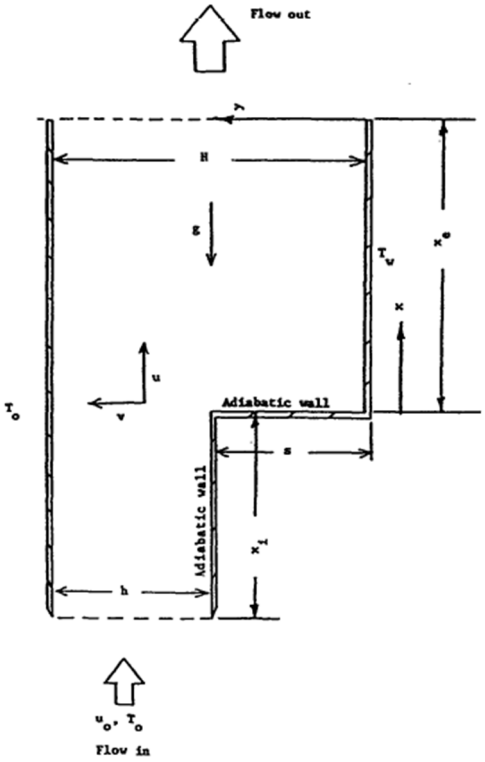

Figure 1 – Schematic representation of the backward-facing step flows

Mathematical formulation of the problem

Consider a two-dimensional laminar convective flow in a vertical channel with a sudden expansion behind the inverse step of height s, as shown in Fig. 1. The straight wall of the channel is maintained at a uniform temperature equal to the temperature of the inlet air T_0. The stepped wall below the stage is heated to a uniform temperature, which can be adjusted to any desired value T_w. The upper part of the stepped wall and the reverse side is installed as an adiabatic surface. The inlet length of the channel x_i and the outlet lower length x_e of the channel are appropriate dimensions. These lengths are assumed to be infinite, but the simulation domain is limited by the length $L_e = x_e + x_i$. The smaller section of the channel before the projection has a height, and the large section below the stage has a height $H = h + s$. Air flows up the channel with mean velocity u_0 and uniform temperature T_0. The gravitational force g in this problem is considered to act vertically downwards.

To describe this physical problem, was used assumption about constant properties, and was used the Boussinesq approximation. This system of equations in an immense form can be written in the form:

1) $$\frac{\partial U}{\partial X}+\frac{\partial U}{\partial Y}=0. \qquad (1)$$

2) $$\frac{\partial U}{\partial t}+U\frac{\partial U}{\partial X}+V\frac{\partial U}{\partial Y}= =-\frac{\partial P}{\partial X}+\frac{1}{\mathrm{Re}}\left(\frac{\partial^2 U}{\partial X^2}+\frac{\partial^2 U}{\partial Y^2}\right)+\frac{Gr}{\mathrm{Re}^2}\theta \qquad (2)$$

3) $$\frac{\partial V}{\partial t}+U\frac{\partial V}{\partial X}+V\frac{\partial V}{\partial Y}= =-\frac{\partial P}{\partial Y}+\frac{1}{\mathrm{Re}}\left(\frac{\partial^2 V}{\partial X^2}+\frac{\partial^2 V}{\partial Y^2}\right) \qquad (3)$$

4) $$\frac{\partial \theta}{\partial t}+U\frac{\partial \theta}{\partial X}+V\frac{\partial \theta}{\partial Y}= =\frac{1}{\mathrm{Pr}\,\mathrm{Re}}\left(\frac{\partial^2 \theta}{\partial X^2}+\frac{\partial^2 \theta}{\partial Y^2}\right) \qquad (4)$$

The dimensionless parameters in the equations given above are defined by the formula:

$$U=u/u_0\,, \qquad V=\upsilon/u_0\,,$$
$$X=x/s\,, \qquad Y=y/s\,,$$
$$\theta=\left(T-T_0\right)/\left(T_w-T_0\right), \qquad P=p/\rho_0 u_0^2\,,$$
$$\mathrm{Pr}=\nu/\alpha\,, \qquad \mathrm{Re}=u_0 s/\nu\,,$$
$$Gr=g\beta\left(T_w-T_0\right)s^3/\nu^2\,.$$

where α – the temperature diffusion, ν – the kinematic viscosity, and β – the thermal expansion coefficient are estimated at the film temperature $T_f=\left(T_0+T_w\right)/2$.

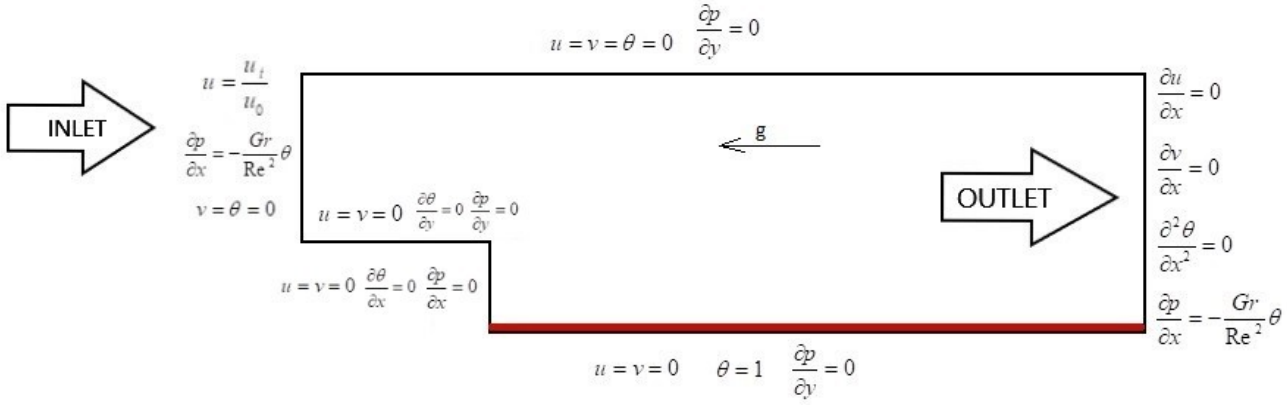

Figure 2 – Boundary conditions

Boundary conditions:

(a) Inlet conditions: At the point $X = -X_i$ and $1 \le Y \le H/s$: $U = u_i/u_0$, $V = 0$, $\theta = 0$, $\frac{\partial p}{\partial x} = -\frac{Gr}{\mathrm{Re}^2}\theta$.
where u_i is the local distribution of velocities at the inlet, which is assumed to have a parabolic profile and u_i/u_0 an average inlet velocity, that is, given by formula

$$u_i/u_0 = 6\left[-y^2 + (H+s)y - Hs\right]/(H-s)^2$$

(b) Outlet conditions: At the point $X = X_e$ and $0 \le Y \le H/s$: $\partial U/\partial X = 0$, $\partial^2\theta/\partial X^2 = 0$, $\partial V/\partial X = 0$, $\frac{\partial p}{\partial x} = -\frac{Gr}{\mathrm{Re}^2}\theta$.

(c) on the top wall: At the point $Y = H/s$ and $-X_i \le X \le X_e$: $U = 0$, $V = 0$, $\theta = 0$, $\frac{\partial p}{\partial y} = 0$.

(d) on the wall of the upper stage: At the point $Y = 1$ and $-X_i \le X < 0$: $U = 0$, $V = 0$, $\partial\theta/\partial Y = 0$, $\frac{\partial p}{\partial y} = 0$.

(e) on the wall of the lower stage: At point $X = 0$ and $0 \le Y \le 1$: $U = 0$, $V = 0$, $\partial\theta/\partial X = 0$, $\frac{\partial p}{\partial x} = 0$.

(f) on the wall below the stage: At the point $Y = 0$ and $0 \le X \le X_e$: $U = 0$, $V = 0$, $\theta = 1$, $\frac{\partial p}{\partial y} = 0$.

The last term on the right-hand side of equation (2) is the contribution of the buoyancy force. The length of the downstream flow from the simulation area was chosen to be 70 steps ($X_e = 70$). The upper length of the design area was chosen to be 5 steps (i.e. $X_i = 5$), and the velocity profile at the input area was set as parabolic profile, like $u_i/u_0 = 6\left[-y^2 + (H+s)y - Hs\right]/(H-s)^2$, and temperature was chosen as uniform T_0.

The numerical algorithm

For a numerical solution of this system of equations, the projection method is used [20-23]. The equations are approximated by the finite volume method [20, 24]. At the first stage it is assumed that the transfer of momentum is carried out only through convection and diffusion, and an intermediate velocity field is calculated by the fourth-order Runge-Kutta method [21, 22]. At the second stage, according to the found intermediate velocity field, there is a pressure field. The Poisson equation for the pressure field is solved by the Jacobi method. At the third stage it is assumed that the transfer is carried out only due to the pressure gradient. At the fourth stage, the equations for the temperature are calculated by the fourth-order Runge-Kutta method [21, 22].

I. $$\int_{\Omega}\frac{\vec{u}^{*}-\vec{u}^{n}}{\Delta t}d\Omega = -\oint_{\partial\Omega}(\vec{u}^{n}\,\vec{u}^{*}-\frac{1}{\mathrm{Re}}\nabla\vec{u}^{*})n_i d\Gamma-\int_{\Omega}\frac{Gr}{\mathrm{Re}^2}\theta d\Omega,$$

II. $$\oint_{\partial\Omega}(\nabla p)d\Gamma=\int_{\Omega}\frac{\nabla\vec{u}^{*}}{\Delta t}d\Omega,$$

III. $$\frac{\vec{u}^{n+1}-\vec{u}^{*}}{\Delta t}=-\nabla p,$$

IV. $$\int_{\Omega}\frac{\theta^{*}-\theta^{n}}{\Delta t}d\Omega=-\oint_{\partial\Omega}(\vec{u}^{n}\,\theta^{*}-\frac{1}{\mathrm{Re}\,\mathrm{Pr}}\nabla\theta^{*})n_i d\Gamma,$$

Parallelization algorithm

For numerical simulation was constructed a computational mesh by using the PointWise software. The problem was launched on the ITFS-MKM software using a high-performance computing. This numerical algorithm is completely parallelized using various geometric domain decompositions (1D, 2D and 3D). Geometric partitioning of the computational grid is chosen as the main approach of parallelization. In this case, there are three different ways of exchanging the values of the grid function on the computational nodes of a one-dimensional, two-dimensional, and three-dimensional mesh. After the domain decomposition stage, when parallel algorithms are built on separate blocks, a transition is made to the relationships between the blocks, the simulations on which will be executed in parallel on each processor. For this purpose, a numerical solution of the equation system was used for an explicit scheme, since this scheme is very efficiently parallelized. In order to use the domain decomposition method as a parallelization method, this algorithm uses the boundary nodes of each subdomain in which it is necessary to know the value of the grid function that borders on the neighboring elements of the processor. To achieve this goal, at each compute node, ghost points store values from neighboring computational nodes, and organize the transfer of these boundary values necessary to ensure homogeneity of calculations for explicit formulas.

Data transmission is performed using the procedures of the MPI library [25]. By doing preliminary theoretical analysis of the effectiveness of various domain decomposition methods of the computational domain for this problem, which will estimate the time of the parallel program as the time T_{calc} of the sequential program divided by the number of processors plus the transmission time $T_p = T_{calc} / p + T_{com}$. While transmissions for various domain decomposition methods can be approximately expressed through capacity:

$$T_{com}^{1D} = t_{send}\,2N^2x2$$

$$T_{com}^{2D} = t_{send}\,2N^2x4p^{1/2} \qquad (5)$$

$$T_{com}^{3D} = t_{send}\,2N^2x6p^{2/3}$$

where N^3 – the number of nodes in the computational mesh, p – the number of processors (cores), t_{send} – the time of sending one element (number).

It should be noted that for different decomposition methods, the data transmission cost can be represented as $T_{com}^{1D} = t_{send}\,2N^2xk(p)$ in accordance with the formula (5), where $k(p)$ is the proportionality coefficient, which depends on the domain decomposition method and the number of processing elements used.

At the first stage, one common program was used, the size of the array from start to run did not change, and each element of the processor was numbered by an array of elements, starting from zero. For the test simulation is used well known problem – 3D cavity flow. Despite the fact that according to the theoretical analysis of 3D decomposition is the best option for parallelization (Figure 3), computational experiments showed that the best results were achieved using 2D decomposition, when the number of processes varies from 25 to 144 (Figure 3).

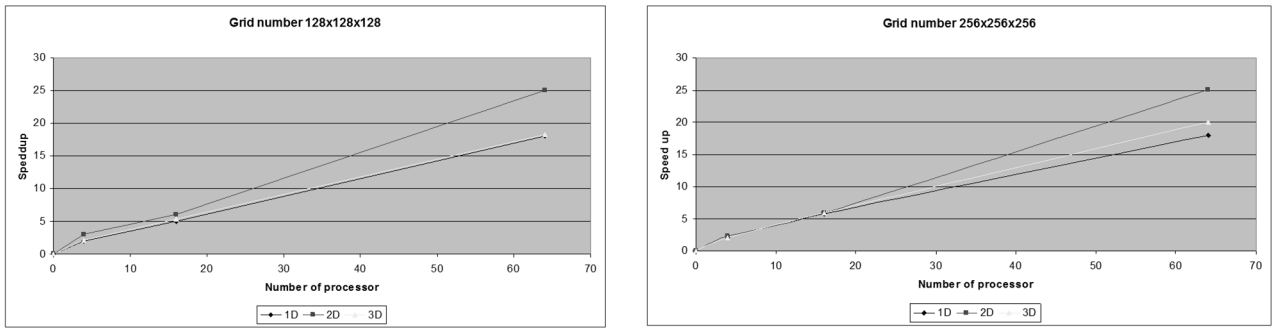

Figure 3 – Speed-up for various domain decomposition methods of the computational domain.

Based on the preliminary theoretical analysis of the graphs, the following character can be noted. The simulation time without the interprocessor communications cost with different domain decomposition methods should be approximately the same for the same number of processors and be reduced by T_{calc}/p. In fact, the calculated data show that when using 2D decomposition on different computational grids, the minimal cost for simulation and the cost graphs are much higher, depending on the simulation time, on several processors taken T_{calc}/p.

To explain these results, it is necessary to pay attention to the assumptions made in the preliminary theoretical analysis of efficiency for this task. First, it was assumed that regardless of the distribution of data per processor element, the same amount of computational load was done, which should lead to the same time expenditure. Secondly, it was assumed that the time spent on interprocessor sending's of any degree of the same amount of data is not dependent on their memory choices. In order to understand what is really happening, the following sets of computational simulations test were carried out. For evaluation, the sequence of the first approach was considered when the program is run in a single-processor version, and thus simulates various geometric domain decomposition methods of data for the same amount of computation performed by each processor.

Numerical results

Geometric parameters are indicated in Figure 1: channel length L = 75, channel height H = 2, step height S = 1. Numerical results were obtained for the dimensionless numbers Re = 50, Pr = 0.7 and Gr = 19.1 [9].

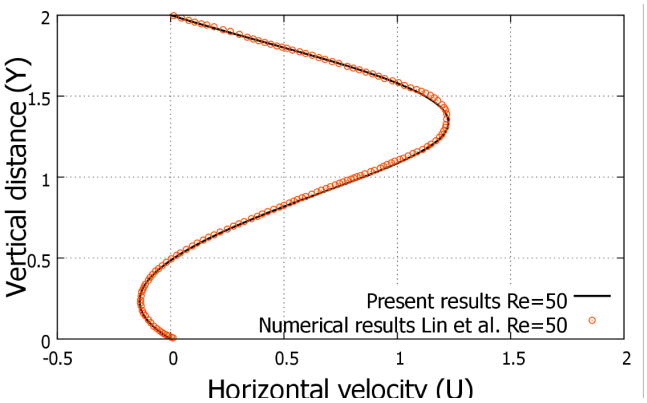

Figure 4 – Velocity profile with vertical buoyancy forces for dimensionless number Re=50, $\Delta T = 1°C$, $x/x_f = 0.5$, where $x_f = 2.91$.

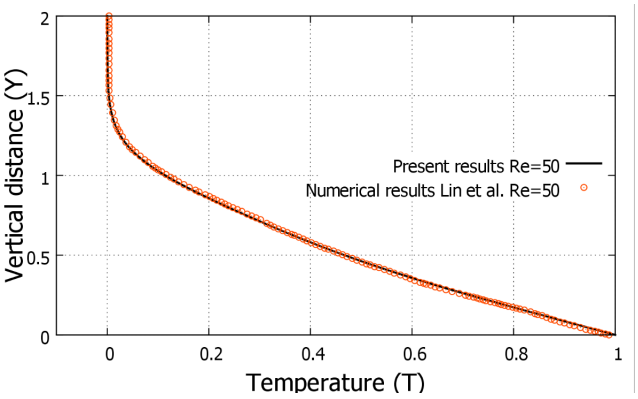

Figure 5 – Temperature profile with vertical buoyancy forces for dimensionless number Re=50, $\Delta T = 1°C$, $x/x_f = 0.5$, where $x_f = 2.91$.

Figure 4 shows the comparison of the longitudinal velocity profile with the numerical data of Lin et al. [9] at the point x/x_f = 0.5,

where $x_f = 2.91$. Figure 5 shows the comparison of temperature profiles with the numerical data of Lin et al. [9] at the point $x/x_f = 0.5$, where $x_f = 2.91$. It can be seen from the figures that the mathematical model and the numerical algorithm which is used in this paper is coincided with the numerical results obtained by Lin et al. [9]. Figure 6 shows the streamlines and the horizontal velocity contour for dimensionless numbers Re = 50, Pr = 0.7 and Gr = 19.1. Figure 7 shows the vertical velocity contour for dimensionless numbers Re = 50, Pr = 0.7 and Gr = 19.1. Figure 8 shows the temperature profile for dimensionless numbers Re = 50, Pr = 0.7 and Gr = 19.1. For a better understanding of this process from figures 6-8 can be seen the development of the backward-facing step flow with vertical buoyancy force: the initiation and process of the development of the region of flows reconnection with taking into account the buoyancy forces.

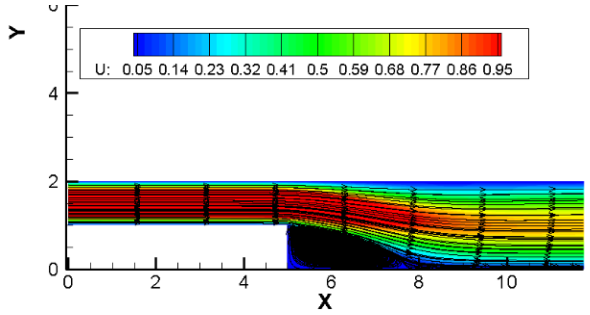

Figure 6 – The contour of the horizontal velocity component with streamlines for dimensionless numbers Re=50, Pr=0.7 and Gr=19.1.

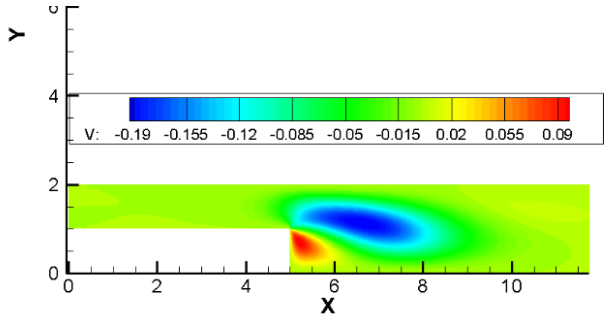

Figure 7 – The contour of the vertical velocity component for dimensionless numbers Re=50, Pr=0.7 and Gr=19.1.

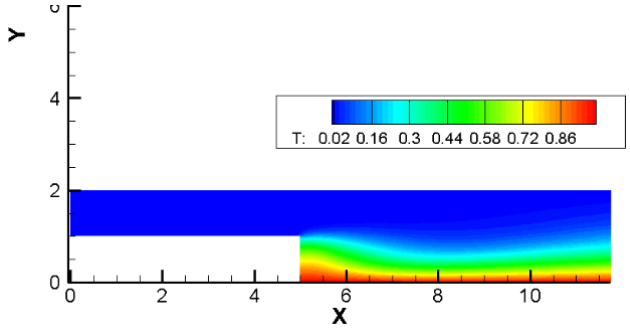

Figure 8 – Temperature contour for dimensionless numbers Re=50, Pr=0.7 and Gr=19.1.

Conclusion

Numerical studies of the laminar flow were carried out by the zone of joining the flows behind the backward-facing step with taking into account the buoyancy forces. This gave a deeper insight into the internal flow behind the backward-facing step and the processes of flows reconnection under the influence of temperature effects, which in turn gave an idea of the further appearance of secondary zones. The distance from the ledge to the canal boundary is 4 times the channel height, for a more detailed study of the backward-facing step flows with taking into account the buoyancy forces [9]. The numerical data of the velocity distribution showed the formation of a primary reattachment zone of backward-facing step flows. To numerically solve the system of Navier-Stokes equations, the projection method was used. From numerical results can be seen that the realized numerical method gives a small error in comparison with the numerical results of other authors [9] for the dimensionless numbers Re = 50, Pr = 0.7 and Gr = 19.1.

Also in this paper is used a parallel algorithm to obtain fast numerical results. This parallel algorithm is based on one-dimensional, two-dimensional and three-dimensional domain decomposition method. The numerical results from the 3D cavity flow test problem, which used 1D, 2D and 3D domain decomposition method showed that 3D domain decomposition is not time-consuming compared to 2D domain decomposition, for the number of processors that does not exceed 250,

and 3D domain decomposition has more time-consuming software implementation and the use of 2D domain decomposition is sufficient for the scope of the problem. That's why for backward-facing step flow with vertical buoyancy force is used 2D domain decomposition. It should also be noted that setting the boundary conditions is an important process. In the future, this mathematical model and a parallel numerical algorithm can be applied to various complex flows taking into account the buoyancy forces.

References

1. Abbott D.E., Kline S.J. Experimental investigations of subsonic turbulent flow over single and double backward-facing steps // J. Basic Engng. – 1962. – Vol.84. – P. 317.

2. Sebanr A. Heat transfer to the turbulent separated flows of air downstream of a step in the surface of a plate // J. Heat Transfer. – 1964. – Vol.86. – P. 259.

3. Goldsteinr J., Eriksenv L., Olsonr M., Eckerte R.G. Laminar separation, reattachment and transition of flow over a downstream-facing step // J. Basic Engng. – 1970. – Vol.92. – P. 732.

4. Durst F., Whitelawj H. Aerodynamic properties of separated gas flows: existing measurements techniques and new optical geometry for the laser-Doppler anemometer // Prog. Heat Mass Transfer. – 1971. – Vol.4. – P. 311.

5. Gosmana D., Punw M. Lecture notes for course entitled: 'Calculation of recirculating flow' // Heat Transfer Rep. – 1974. – Vol.74. – P. 2.

6. Kumara, Yajnikk S. Internal separated flows at large Reynolds number // J. Fluid Mech. – 1980. – Vol.97. – P. 27.

7. Chiang T.P., Tony W.H., Sheu, Fang C.C. Numerical investigation of vortical evolution in backward-facing step expansion flow // Appl. Math. – 1999. – Vol.23. – P. 915-932.

8. Fletcher C.A.J. Computational techniques for fluid dynamics 2 // Springer-Verlag New York. – 1988. – Vol.1. – P. 387.

9. J.T. Lin, B.F. Armaly, T.S. Chen. Mixed convection in buoyancy-assisting, vertical backward-facing step flows. // International Journal of Heat and Mass Transfer. – 1990. – Vol. 33, Issue 10. – P. 2121-2132.

10. B. F. Armaly and F. Durst, Reattachment length and recirculation regions downstream of two dimensional single backward facing step. In Momentum and Hear Transfer Process in Recirculating Flows, ASME HTD. – 1980. – Vol. 13. – P. l-7.

11. J. K. Eaton and J. P. Johnson, A review of research on subsonic turbulent flow reattachment, AfAA J. – 1981. – Vol. 19. – P. 1093-1100.

12. R. L. Simpson. A review of some phenomena in turbulent flow separation, J. Fluid Engng. – 1981. – Vol.103. – P. 52-530.

13. W. Aung, An experimental study of laminar heat transfer downstream of backsteps, J. Heat Transfer. – 1983. – Vol.105. – P. 823-829.

14. W. Aung, Separated forced convection, Proc. ASMEIJSME Thermal Enana Joint Con/ ASME. New York. – 1983. – Vol. 2. – P. 499-515.

15. W. Aung, A. Baron and F. K. Tsou, Wall independency and effect of initial shear-layer thickness in separated flow and heat transfer, Int. J. Hear Muss Transfer. – 1985. – Vol. 28. – P. 1757-1771.

16. W. Aung and G. Worku, Theory of fully developed. Combined convection including flow reversal, J. Hear Transfer. – 1986. – Vol. 108. – P. 485-488.

17. E. M. Sparrow, G. M. Chrysler and L. F. Azevedo. Observed flow reversals and measured-predicted Nusselt numbers for natural convection in a one-sided heated vertical channel, J. Heat Transfer. – 1984. – Vol. 106. – P. 325-332.

18. E. M. Sparrow, S. S. Kang and W. Chuck. Relation between the points of flow reattachment and maximum heat transfer for regions of flow separation. Inr. J. Hear Mass Transfer. – 1987. – Vol. 30. – P. 1237-1246.

19. E. M. Sparrow and W. Chuck, PC solutions for heat transfer and fluid flow downstream of an abrupt, asymmetric enlargement in a channel, Numer. Hear Transfer. – 1987. – Vol. 12. – P. 1940.

20. Chung T.J. Computational fluid dynamics. – 2002. – P. 1034.

21. Issakhov A., Mathematical modeling of the discharged heat water effect on the aquatic environment from thermal power plant // International Journal of Nonlinear Science and Numerical Simulation, – 2015. – Vol. 16(5). – P. 229–238, doi:10.1515/ijnsns-2015-0047.

22. Issakhov A., Mathematical modeling of the discharged heat water effect on the aquatic environment from thermal power plant under various operational capacities // Applied Mathematical Modelling, – 2016. – Vol. 40, Issue 2. – P. 1082–1096,

http://dx.doi.org/10.1016/j.apm.2015.06.024.

23. Issakhov A. Large eddy simulation of turbulent mixing by using 3D decomposition method // *J. Phys.: Conf. Ser.* – 2011. – Vol. 318(4). – P. 1282-1288, doi:10.1088/1742-6596/318/4/042051.

24. Chorin A.J. Numerical solution of the Navier-Stokes equations // Math. Comp. – 1968. – Vol. 22. – P. 745-762.

25. Karniadakis G. E., Kirby II R. M. Parallel Scientific Computing in C++ and MPI: A Seamless Approach to Parallel Algorithms and their Implementation. Cambridge University Press. – 2000. – P. 630.

26. Ngo I., Byon C., Effects of heater location and heater size on the natural convection heat transfer in a square cavity using finite element method, J. Mech. Sci. Technol. – 2015. – Vol. 29 (7). – P. 2995.

27. Oztop H. F., Abu-Nada E. Numerical study of natural convection in partially heated rectangular enclosures filled with nanofluids, Int. J. Heat. Fluid Fl. – 2008. – Vol. 29 (5). – P. 1326-1336.